THE JOURNAL OF PHYSICAL CHEMISTRY C

Article

pubs.acs.org/JPCC

Mechanisms Underlying the Mpemba Effect in Water from Molecular Dynamics Simulations

Jaehyeok Jin[†,∥] and William A. Goddard, III*[,‡,§]

[†]Department of Chemistry and [‡]Graduate School of EEWS, Korea Advanced Institute of Science and Technology, Daejeon 305-701, Korea

[§]Materials and Process Simulation Center (MC 139-74), California Institute of Technology, 1200 East California Boulevard, Pasadena, California 91125, United States

Supporting Information

ABSTRACT: Experimentally, quenching from warmer water leads to faster freezing than quenching from colder water—the Mpemba effect. Using molecular dynamics, we find that quenching water from 370 K and above leads to a 100 K density of states (DOS) closer to that of ice than quenching from 300 K and below. Especially we find that the biggest difference is for 80−160 cm^{-1} which upon quenching from colder water is much lower than that in ice, while it is much higher than in ice when quenching from warm water. We find that the range of 100−160 cm^{-1} corresponds to framework vibrations within a hexamer, suggesting that the water hexamer serves as a nucleus for crystallization. We tested this by fixing one hexamer and quenching slowly from 370 K, leading to increased correlation with pure ice. We also showed that the structure quenched from 370 K evolves to the ice faster than 300 K case. These results suggest that the higher population of water hexamer states in warm water is responsible for the faster crystallization underlying the Mpemba effect.

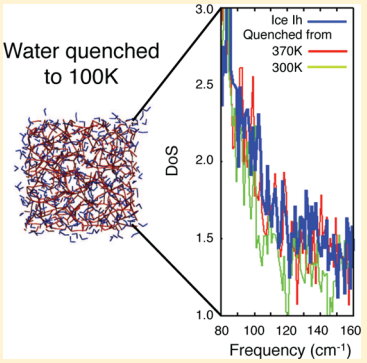

1. INTRODUCTION

The Mpemba effect occurs when two bodies of water, identical in every way, except that one is at a higher temperature than the other, are exposed to identical subzero surroundings, and the initially hotter water freezes first. This effect, which seems irrational at the first glance, has been observed in numerous experiments.[1,2] Recently, it has also been observed that structural changes in supercooled water can affect the crystallization properties of ice.[3,4] However, a convincing atomistic explanation of the Mpemba effect has not yet been advanced.[2−6]

In this work, we carried out molecular dyanmics (MD) studies using several force fields to examine the effect of quenching water from a range of temperatures, aimed at understanding the origin of the Mpemba paradox.

2. CALCULATION DETAILS

To describe the cooling behavior of water[7−9] we carried out MD simulations (using the LAMMPS simulation package) for systems with 192, 300, and 1000 water monomers.[10] We considered three force field models: (i) The single bead Molinero model, mW,[7] which uses a Stillinger−Weber angular function to retain tetrahedral character, but has no internal water structure. (ii) The SPC rigid water model,[8] which has internal water structure, but is not flexible. (iii) The F3C flexible water model,[9] which has both internal water structure and explicit motions of the HO bonds and angles.

The mW coarse-grained model leads to computational costs of 1/3 that of the others; however, it ignores the rotational libration modes. We find that the SPC and F3C models have quite similar vibrational density of states (DOS) for translational and rotational libration, but we focused our analysis on the more flexible F3C model on the chance that the OH vibrations might have some influence. Detailed comparisons and descriptions of the size of system and force fields are discussed in section 3.2. To validate the accuracy of the DOS from the F3C force field, we compare it to the experimental DOS of ice. There are more than 15 distinct phases of the ice at various temperatures and pressures,[11,12] but ice Ih, V, and II are relevant for comparing to our MD simulations, which were performed at pressures of 0−0.1 GPa.[13] The vibrational DOS from the two-phase thermodynamics (2PT) analysis[14,15] of the dynamics using the F3C model reproduces well the experimental DOS of the ice Ih crystal, and the DOS from the very accurate WHBB (Wang/Huang/Braams/Bowman) potential derived from accurate QM calculations,[16,17] as shown in Figure 1. The experimental spectra of ice Ih show the following: (i) A peak at 600−1000 cm^{-1} that can be understood in terms of vibrations of the 12-molecule unit cell.[18] This peak also appears in the 2PT analysis of the F3C force field and for the WHBB potential, but it extends down to about 400 cm^{-1}.[16] (ii) Sharp peaks near 220 and 300 cm^{-1} with a smaller peak at 150 cm^{-1}. The WHBB potential leads to two peaks over the same region, and the F3C leads to a broad peak covering the

Received: November 24, 2014
Revised: January 9, 2015
Published: January 14, 2015

DOI: 10.1021/jp511752n
J. Phys. Chem. C 2015, 119, 2622−2629

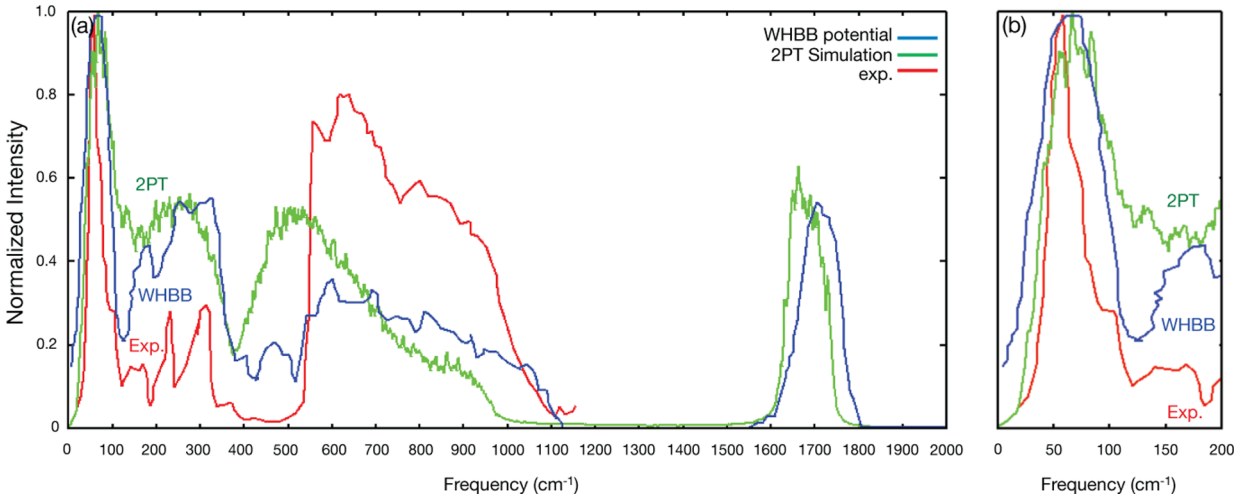

Figure 1. DOS from the 2PT analysis of the F3C MD on ice Ih (green) compared to experiment (red) and the WHBB potential (blue): (a) full spectrum to 2000 cm^{-1} and (b) magnified comparison from 0 to 200 cm^{-1}.

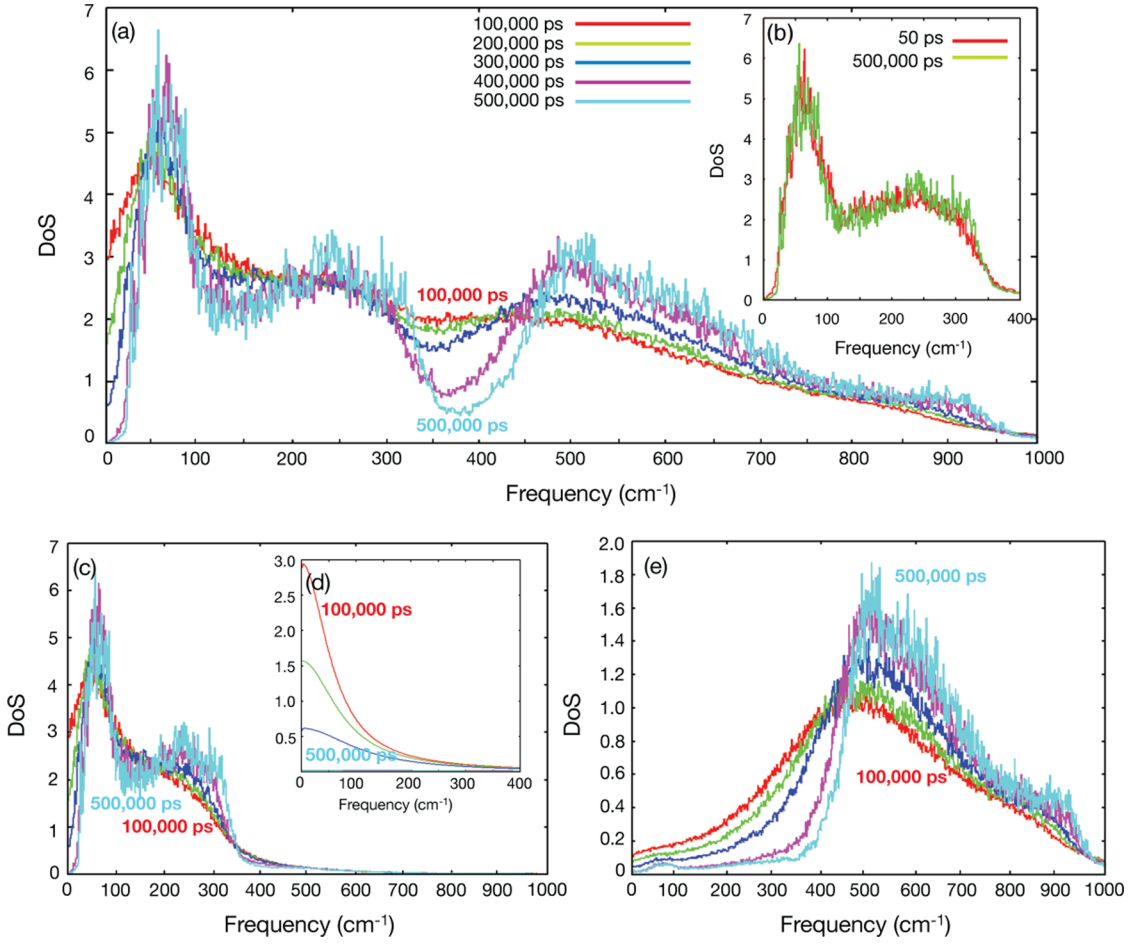

Figure 2. Changes in the vibrational DOS as the system is quenched over 500 ns from 2PT analysis using the F3C FF. (a) Changes in the total DOS while quenching from 370 to 100 K over a period of 500 ns. (b) Comparison of the final translational libration DOS for quenching times with that from quenching in 50 ps and 500 ns. (c) Translational libration DOS. (d) Diffusional component (hard-sphere gas-like) of the DOS. (e) Rotational libration DOS.

same region. These modes are known as transverse optic vibrations (229 cm^{-1}) and longitudinal acoustic vibrations (164 cm^{-1}) from inelastic neutron scattering (INS) experiment and transverse optic vibrations of the six-member rings from WHBB potential.[16,19] (iii) A strong peak at 60 cm^{-1} also exhibited by both WHBB and F3C. This corresponds to the acoustic translational mode of the six-member rings from analysis of the WHBB potential.[16,19]

DOI: 10.1021/jp511752n
J. Phys. Chem. C 2015, 119, 2622−2629

Thus, we find that the 2PT predicted vibrational DOS is consistent with INS experiments and with the ab initio potential surface calculations.[16,17]

3. RESULTS AND DISCUSSIONS

3.1. Explanation of the Mpemba effect. *3.1.1. Changes in DOS from Fast Quenching to 100 K from Various Temperatures.* To examine the Mpemba effect, we started with an equilibrated water box with 192 molecules at various temperatures from 280 to 390 K which we then quenched rapidly to 100 K with NVT dynamics. (The original observations of the Mpemba compared quenching from 305 and 373 K.[20]) Since the experimental time scales are much longer than the simulations, we considered quenching times ranging from 50 ps to 500 ns and calculated the evolution of the DOS as shown in Figure 2 and Figures S3–S6 of the Supporting Information (SI).[21−23] We see little difference over the whole range and concluded that the quenching time of 2 ns leads to the most suitable case for comparing the supercooled state quenched from various initial temperatures. Recently, Malaspina and co-workers studied the properties of supercooled water using four water models and concluded that a 2 ns time scale led to converged predictions of properties.[24]

Figure 2 shows the evolution of the DOS, quenched from 370 to 100 K over the period of 500 ns. Figure 2b shows that the final translational libration DOS at 100 K after quenching in 50 ps is very similar to that from quenching over 500 ns.

Table 1 shows the correlation coefficient of the 2PT DOS from various total quenching times with the DOS of normal ice.

Table 1. Correlation Coefficient of Dos Value between Pure Ice Ih and Supercooled Waters Quenched from 370 to 100 K for Different Quenching Times[a]

	correlation coefficient with pure ice Ih at 100 K		
quenching time (ps)	hard-sphere DOS	translational DOS	rotational DOS
50	0.9896	0.9677	0.9861
500	0.9944	0.9694	0.9837
5000	0.9994	0.9692	0.9783
50 000	0.9998	0.9705	0.9713
500 000	0.9997	0.9654	0.9687

[a]This correlation coefficient is calculated by the covariance matrix.

We conclude that the character of the final supercooled DOS from the 500 ns quench is captured with the 50 ps quenching time. (The SI shows the DOS at 100 K for water quenched over these various periods.)

3.1.2. Identification of Critical Part of DOS for Rapid Crystallization. In order to understand the differences in quenching from various temperatures, we partition the total DOS into three parts: (1) The diffusional or hard sphere contribution (see Figure 2d inset to Figure 2c) that decreases exponentially from 0 to 200 cm^{-1} and whose amplitude decreases rapidly to 0 as the liquid water is quenched to form the glass. (2) The translational libration contribution (Figure 2c) ranging from 0 to 400 cm^{-1} is composed of two parts 0–100 cm^{-1} and 100–320 cm^{-1}. As the system is quenched, the DOS decreases in the range of 90–160 cm^{-1} and increases in the range 160–320 cm^{-1}. (3) The rotational libration contribution (Figure 2e) at 370 K goes from 0 to 900 cm^{-1} with the peak at 400 cm^{-1}. Upon quenching, this peak decreases dramatically below 400 cm^{-1} with the peak moving to 450 cm^{-1} and the 450–900 cm^{-1} region growing rapidly with time.

The overall DOS depicted in Figure 2a results from summing these components. The rapid decrease over the range from 250 to 400 cm^{-1} results from the decline of both solidlike translational libration and rotational libration in this region.

To focus on the changes in the DOS upon quenching from various temperatures, Figure 3a compares the translational libration DOS of the supercooled liquid at 100 K with the initial DOS at 370 K, while Figure 3b does the same for the 300 K case. Here we identify three regimes: (I) Region I ranges from 0 to 80 cm^{-1}. This is mostly related to the solidlike behavior as described by the Debye model.[25] Here the gaslike or diffusional DOS is high in the liquid, but drops quickly to zero with supercooling to the glassy state. (II) Region II ranges from 80 to 160 cm^{-1}. Here the DOS decreases but the decline depends on the total quenching time and the starting temperature (see SI Figure S2). (III) Region III ranges from 160 to 400 cm^{-1}. Here the DOS increases slightly up to 300 cm^{-1} and drops to zero above 300 cm^{-1}. We see little differences for initial temperatures of 300 and 370 K.

Since regime II depends on the initial temperature and on the quenching rate, we analyzed it further as follows:

In order to interpret the DOS of supercooled water with the DOS for the ice structure, Table 2 compares the correlation coefficients. First, we obtained a smooth spectrum using cubic

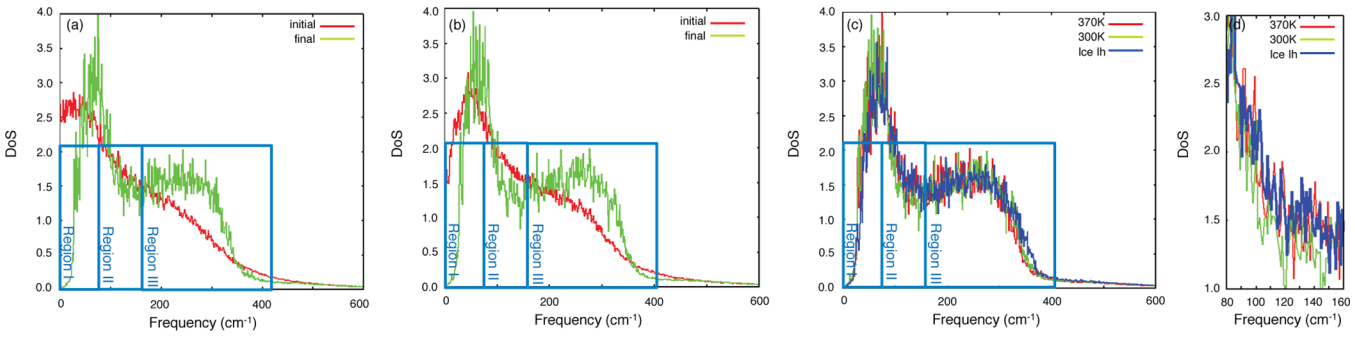

Figure 3. Comparison of the translational libration DOS for water and the DOS after supercooling to 100 K over 2 ns: (a) 370 K initial temperature and (b) 300 K initial temperature as region I from 0 to 80 cm^{-1}, region II from 80 to 160 cm^{-1}, and region III from 160 to 400 cm^{-1}. (c) Comparison of quenched states from both 300 and 370 K to 100 K ice Ih (comparison on 50 ps run is held in Figure S7). (d) Magnified comparison of quenched states and ice Ih in region II.

DOI: 10.1021/jp511752n
J. Phys. Chem. C 2015, 119, 2622−2629

Table 2. Correlation Coefficient of Water Supercooled Quenched of 2, 50, and 50 ns from Various Initial Temperatures[a]

	(a) 2 ns			(b) 50 ps			(c) 50 ns		
	region			region			region		
initial T (supercooled)	I	II	III	I	II	III	I	II	III
280 K	0.9312	0.6812	0.9351						
300 K	0.9724	0.7649	0.9408	0.8685	0.8673	0.9611	0.9043	0.7738	0.9426
335 K	0.9388	0.7453	0.9445	0.9527	0.8794	0.9261	0.9462	0.9101	0.9603
355 K	0.9837	0.7907	0.9472	0.9054	0.8844	0.9572			
370 K	0.9534	0.8723	0.9472	0.9283	0.9123	0.9588	0.9385	0.9257	0.9527
390 K	0.9354	0.8891	0.9530	0.9804	0.9096	0.9275			

[a]The correlation coefficient is calculated by the covariance matrix of a smooth spectrum.

splines and then compared the cases of supercooled water quenching over 2 ns from initial temperatures of 280, 300, 335, 355, 370, and 390 K with spectrum of 100 K pure ice Ih.

For the 2 ns quench, we see that quenching from temperatures of 370 K and higher leads to a high correlation (0.87−0.95) to ice in all three regimes, whereas cooling from 335 K and below leads to a low correlation (0.68−0.76) for regime II. For the 500 ns quench, only the 300 K case has a low correlation with ice, while for the 50 ps case the correlations with quenching from various temperatures is not as marked. Detailed DOS of supercooled water quenched from 300 and 370 K is depicted in Figure S7 with comparison to the DOS of ice.

These results suggest that the there is something important about region II for forming ice. At 370 K and above, there are more states here than in ice, suggesting that the modes in this region are important in nucleating ice formation. This contrasts with the DOS obtained quenching from 335 K and below where there are fewer states in region II than in ice. Thus, for 2 ns quenches, there is clear difference in region II between ≤300 and ≥370 K. For the 50 ns quenches, we still see the dramatic difference between ≤300 and ≥370 K. This suggests that the slower formation of ice when quenching from the lower temperature is related to building up the states in regime II to the level needed for which nucleation of ice can occur. This then is the origin of the Mpemba effect.

3.1.3. Interpretation of the Mode Character for Region II. In order to identify which structural characteristics of water might correspond to regime II, we artificially decreased the mass of selected oxygen atoms from 16 to 2 for three cases: (1) one hexagon of waters from the ice Ih structure, (2) one fused hexagon (a decagon) of waters from the ice Ih structure, and (3) two distinct hexagons of waters from the ice Ih structure.

This led to the DOS shown in Figure 4, where three peaks were observed. These are denoted as 1, 2, and 3 and distributed over the range of 170−350 cm^{-1} (see circles in Figure 4). To compare these results with the DOS for normal water, we scale by SQRT(4/18), leading to 80, 110, and 160 cm^{-1} for peaks 1, 2, and 3, respectively. This is the same as regime II. In contrast differences between these three DOSs in the range higher than 350 cm^{-1} quite small. Also, in the low frequency region below 100 cm^{-1}, entangled DOSs are observed which is known as the pattern of acoustic translations of H_2O.[16,19] Detailed explanations are provided in section E of the SI. However, as Table 2 and Figure S8 indicate, we will restrict our investigations to regime II.

Correcting peak 1 at 169 to 186 cm^{-1} in Figure 4 (a dashed circle) by SQRT(4/18) shifts the peak to the range of 80−88 cm^{-1}. Comparing the DOS of these three cases with ice Ih

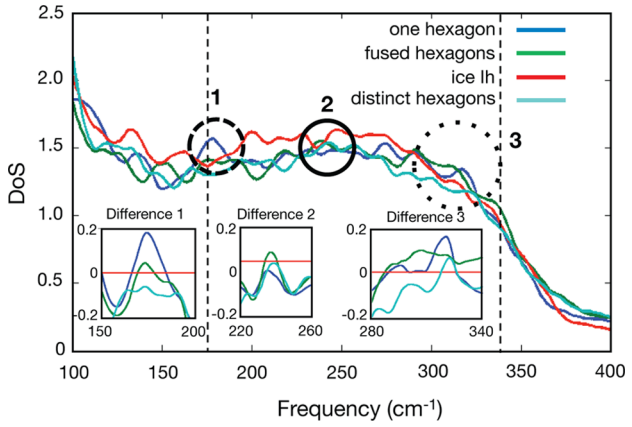

Figure 4. Translational libration DOS of supercooled water at 100 K quenched from 370 K over 2 ns for 3 cases in which the masses of selected waters have the mass of oxygen changed from 16 to 2 amu. These are a hexagon (blue), a fused decamer (green), or two distinct hexagons (cyan): Also shown are the differences between the DOS for these three cases with that of the ice Ih at each peak.

shows that peak 1 is mostly associated with the internal vibrational modes of a water hexamer and/or the water fused decamer, but not with distinct hexagons. A similar trend is found for peak 3 (a dotted circle) in the range of 290−327, which after correcting for the masses corresponds to 137−154 cm^{-1}. However, peak 2 from 234−240 cm^{-1} (a solid circle) which corresponds to 110−113 cm^{-1} is mainly associated with the fused hexagonal motion of the water, not with separate hexagonal motions from water. This suggests that the water hexamer and/or fused hexagons may serve as a nucleus for ice formation.

Thus, from Figure 4, we conclude that quenching warm water leads to a much higher fraction of water hexamer and fused decamer modes than bulk ice, which can then relax quickly to form the crystal. In contrast, quenching from cool water leads to a much smaller fraction of water hexamer and water fused decamer modes, whose populations must increase while forming ice. We conclude that the hexamer and/or the fused decamer are critical nuclei for ice formation and that cooling from cold water leads to too few of these critical clusters. Instead they must build up to form the crystal, slowing the process. The idea here is that at lower temperatures the completion of hydrogen bonding between waters in adjacent hexagons might be more important than those within the hexagon, reducing the number of pure hexamer modes, whereas at high temperatures the fluctuations may randomize these interhexagon modes so important in ice.

DOI: 10.1021/jp511752n
J. Phys. Chem. C 2015, 119, 2622−2629

3.1.4. Role of Hexamer and Fused Defamer in Crystallization. In order to analyze further the modes of waters to be ascribed to ice formation, we interpolated the local DOS using a cubic polynomial to obtain the noiseless spectral density shown in Figure 5.

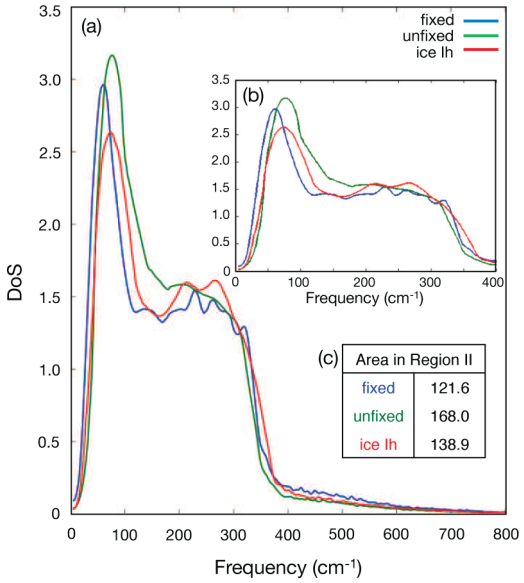

Figure 5. Translational libration DOS in regime II (80−160 cm^{-1}) for water quenched to 100 K from 370 and 300 K at four total quench times ranging from 0.2 to 20 ns.

This shows that the DOS at 100−160 cm^{-1} is generally much higher when quenching from 370 K than the DOS of water supercooled from 300 K, even for the modest total quench time of 0.5 ns. In Figure 4, we identified three major peaks (80−88, 110−113, and 137−154 cm^{-1}) whose effective motions might underlie the Mpemba effect: Here, the local DOS for various total quench times indicate that the two motions, 110−113 and 137−154 cm^{-1}, are crucial, suggesting that water hexamers or decamers are responsible.

To test further the idea that the presence of a large number of water hexamers in warm water compared to cool might increase the rate of crystallization, we took the water hexamer structure obtained by MD with the 6 low mass oxygens, fixed all 18 atoms of these waters, and then heated the whole system (except for these 6) to 370 K and quenched to 100 K. These results are shown in Figure 6.

We calculated the area under each curve of three cases in regime II (using the trapezoidal approximation), leading to the areas in Figure 6c. We see that the fixed case leads to an area similar to ice Ih but that the unfixed case is much larger. This significant increase in the correlation for region II, indicates that water hexamer modes in the region II play an important role in the biasing the high temperature water toward the ice structure.

3.2. Simulation Details and Discussions. *3.2.1. Discussions on the Simulation Settings.* We prepared water molecules with N = 192, 300, and 1000 monomers from the Amorphous builder module of Cerius2. A system with 1000 H_2Os was used in the simulation to compare three water force fields. To ensure that each system size gives reliable properties, we compare the translational librational DOS of the supercooled water from 370 to 100 K for 50 ps from three different system sizes; see Figure 7a. The system with 1000 monomers was used in comparison with other force fields with F3C. The system with 300 monomers was used for extended time scale simulations of quenching times from 500 ps to 500 ns and for interpolation of local DOS (subsections 3.1.1 and 3.1.4). Finally, the system with 192 monomers was used for numerous

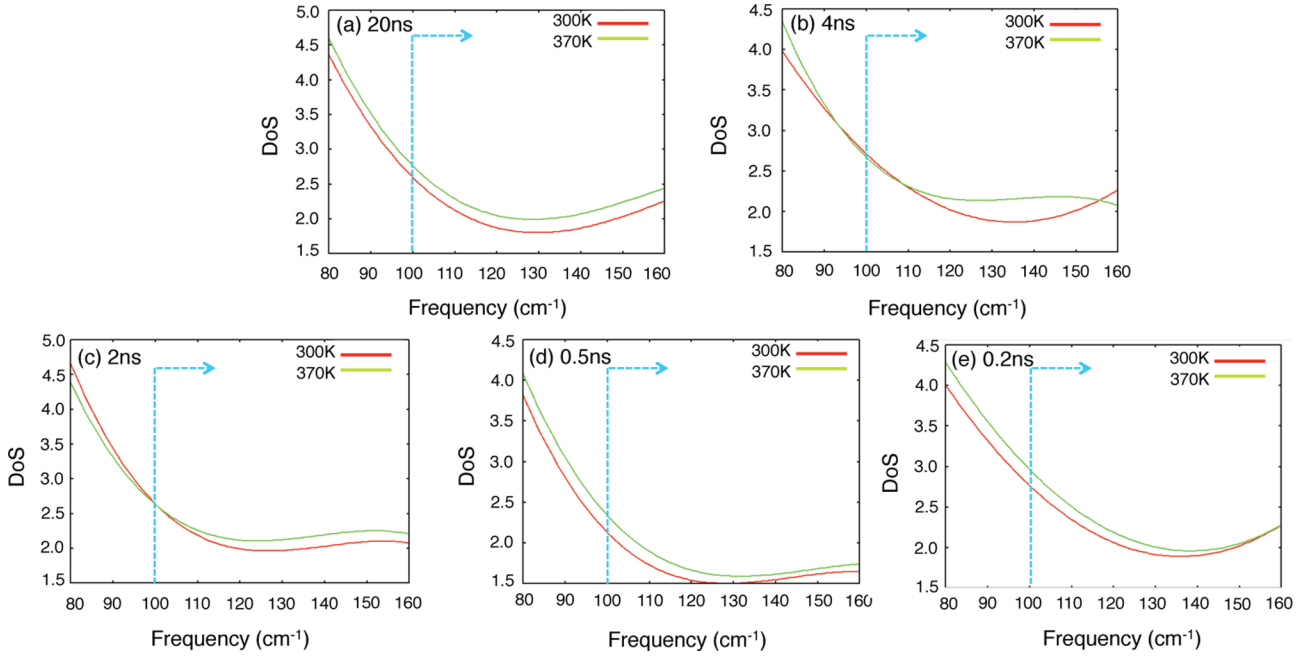

Figure 6. Test of the water hexamer nucleus seed hypothesis. Comparison with ice Ih (red) of the translational libration DOS of supercooled water at 100 K after quenching from 370 K for two cases: (1) *Unfixed*. Here all waters have normal masses (green). (2) *One hexamer* of waters are fixed from the previous calculation using reduced O masses (blue). This system was heated from 100 to 370 K over 50 ps, equilibrated for 200 ps, and then quenched to 100 K over a period of 2 ns. (a) Translational libration DOS to 900 cm^{-1}. (b) Magnified comparison from 0 to 400 cm^{-1} (c) Areas of region II under each curve.

DOI: 10.1021/jp511752n
J. Phys. Chem. C 2015, 119, 2622−2629

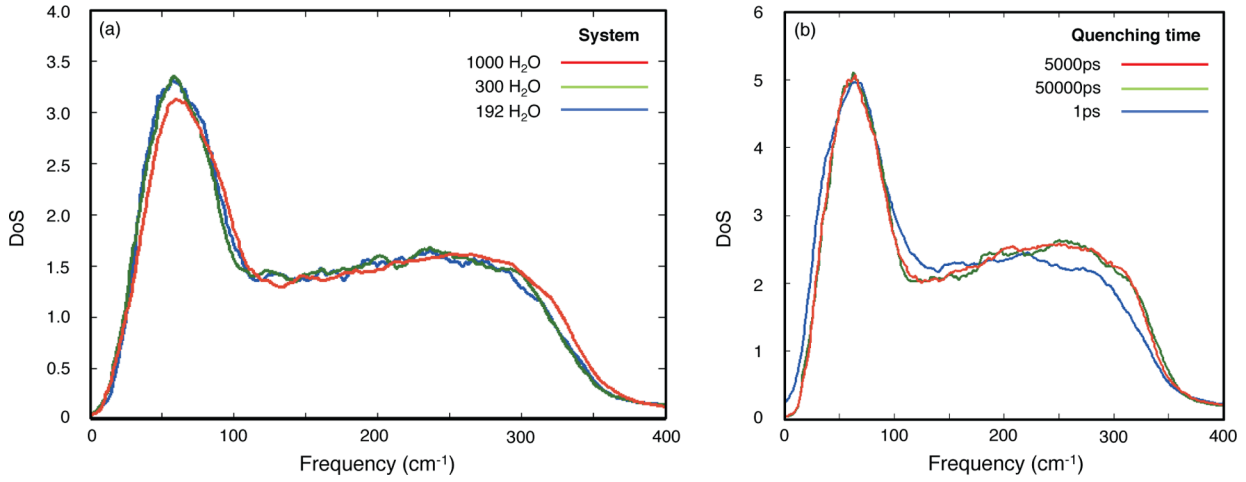

Figure 7. Translational libration DOS for various quenching times and various system sizes. (a) Comparison of the scaled DOS among systems with various numbers of water monomers: Systems with 192, 300, and 1,000 H_2Os. (b) Comparison of the DOS from quenching from 370 to 100 K over times ranging from 1 ps to 5000 and 50 000 ps for the system with 300 water monomers.

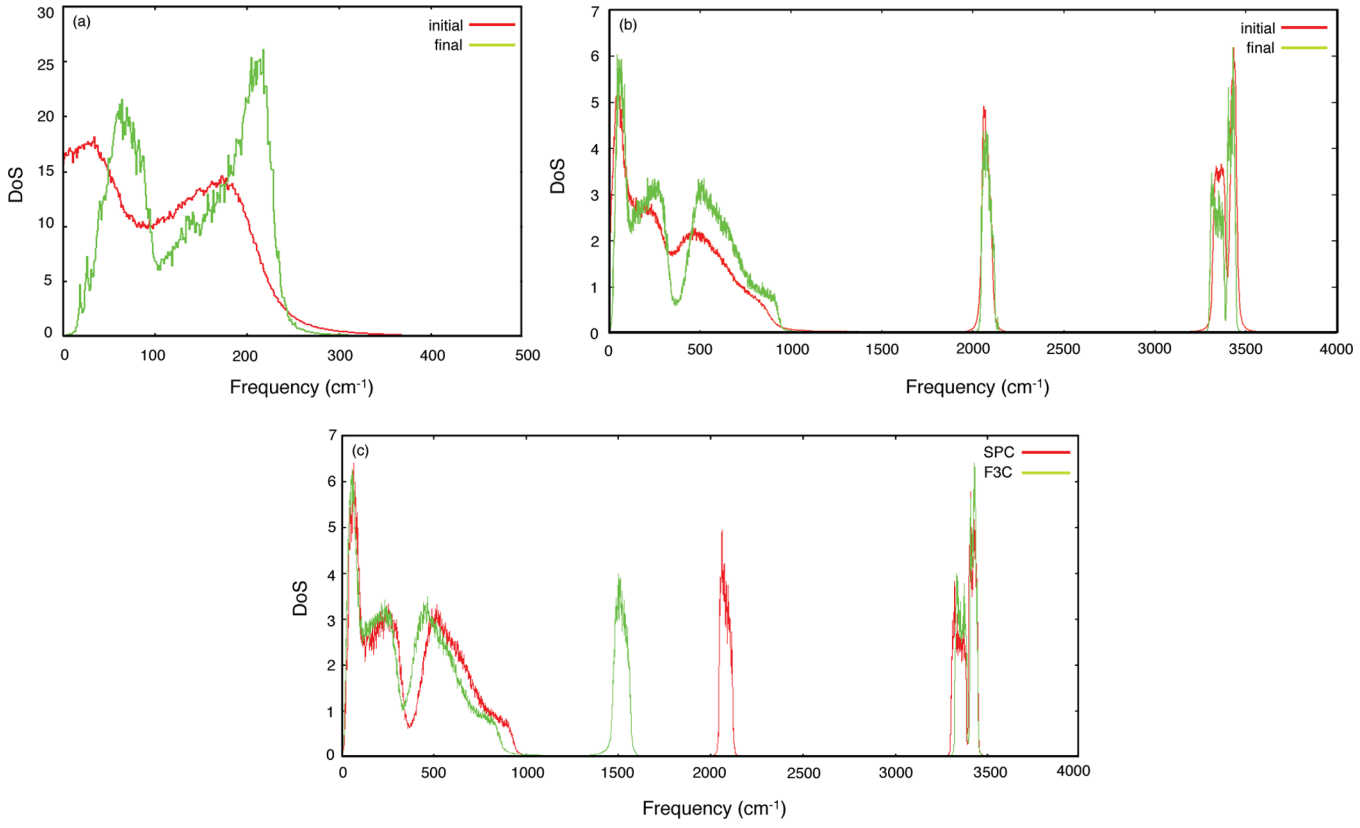

Figure 8. Evolution of DOS of the supercooledwater from 300 to 100 K represented by three different force fields: mW, SPC, and F3C. (a) Initial and final total DOS by using mW model. (b) Initial and final total DOS by using SPC model. (c) Comparison of final total DOS of SPC and F3C model.

quenching studies starting from various temperatures between 280 and 390 K and for the modified mass simulation (subsections 3.1.2 and 3.1.3).

First, we annealed the system at the initial temperature (ranging from 280 to 390 K) and performed constant pressure dynamics with a Nosé-Hoover thermostat and Andersen barostat (NPT) at the desired initial temperature. While quenching, we carried out constant volume dynamics with a Nosé-Hoover thermostat using a 0.1 ps damping constant.

Water exhibits negative thermal expansion between 273 and 277 K, and the cubic ice structures show a negative thermal expansion at <73 K, which is not included in our range.[26] However, to ensure the equilibrated states, we checked that the pressure converged to positive and ambient condition and also the final densities after the calculation in Figure 7a were within the range from 1.09 to 1.12 for all three systems. Finally, after the system is equilibrated, 2PT calculation was conducted by a single short MD dynamics for 20 ps to determine the DOS of the system.

DOI: 10.1021/jp511752n
J. Phys. Chem. C 2015, 119, 2622−2629

3.2.2. Discussions on the Time Scale of the Simulation. We used the periodic cell composed of 300 water monomers with size of 2.08 nm × 2.08 nm × 2.08 nm to perform the extended quenching time simulations from 500 ps to 500 ns, whereas typical experiments may consider quenching times of seconds. This raises the question about whether the simulations could catch the distinctions observed experimentally.

We argue that the simulations can describe the distinctions observed experimentally for much longer time scales. The reason is that the simulations use periodic boundary conditions that introduces long distant correlations not present in the experiment. The speed of sound in water is 1.5 km/s (1.5 nm/ps). Thus, with our periodic cell of 2.08 nm (300 waters), the time scale for the system to change its ordering from that of 370 or 300 K water to that of supercooled water is some multiple of the time 1.39 ps needed for energy to flow throughout the periodic cell. Because of periodic boundary conditions, the long-range ordering over a centimeter is achieved in the same time. In contrast, for an experimental study on a system with a size of 1 cm, it might take 5×10^6 times longer, or a multiple of 6.6 μs to order.

Indeed, our results in Table 1 show little difference in the overall DOS for quenches ranging from 50 ps to 500 ns. Thus, our quenching study over 500 ns may correspond to time scale for a 1 cm system of order 25 s.

On the other hand, for simulation time less than some multiples of 1.39 ps, we might expect to see differences. Indeed the blue line in Figure 7b is for a quench time of 1 ps, and we see a dramatic difference compared to quenching times of 5 and 50 ns.

3.2.3. Comparison of Different Force Fields. The detailed comparison between the DOS for various force fields is depicted in Figure 8.

Figure 8a leads to the quenched DOS from the mW model. This necessarily ignores the rotational contribution to the DOS, leading to major differences in the quenched DOS compared within Figure 1.

Figure 8b shows the evolution of DOS for the SPC rigid water model, while quenching. We see that SPC leads to a similar DOS for the vibrational regions as F3C (Figure 8c), so that its use to examine the Mpemba effect might well have been sufficient. However, to examine the possible influence of the OH vibrations, we used the F3C model for our studies. This allowed us to more convincingly analyze the region affected by the hexagonal modes.

4. SUMMARY

In order to understand the origin of the Mpemba effect, we carried out molecular dynamics simulations to investigate how quenching from various initial temperatures might affect crystallization of supercooled water. In particular, we considered quenching to 100 K from various temperatures ranging from 280 to 390 K, using the 2PT analyses to obtain the vibrational density of states (DOS). From these DOS, we identified that the population in regime II (80−160 cm^{-1}) plays an important role in crystallizing ice. That is quenching from warm water (above 370 K) has a higher population than ice in this region, which can then simply relax to the values of ice, while quenched water quenched from cool water (below 300 K) has a lower population than ice in this region, which must slowly be built up to form ice. This explains the Mpemba effect.

In order to interpret what is special about the DOS in the 80−160 cm^{-1} region, we carried out calculations in which hexagons or decagons of water had modified masses. This allowed us to conclude that regime II is associated with internal vibrations of water hexagons or perhaps fused decagons.

We then analyzed the modes of ice as it melts where again we identified regime II with hexagons of water (or perhaps fused decagons). Here we showed that fixing one of these hexagons and quenching from 370 K leads to faster crystal growth than that for fully free water, and that quenching from 300 K leads also to faster crystal growth. This supports the hypothesis that the water hexamer plays an important role in nucleating ice formation

Thus, the explanation of the Mpemba effect is that warm water has a higher population of the water hexagon ice nuclei than that in ice, whereas for cooler water this hexagon population is below that of ice (due to increased hydrogen bonding between waters in different hexamers in low temperature water). The remaining question is why the hexagon population is higher for high temperature water. We conjecture that at high temperature the intrahexamer modes decouple from interhexagon motions, leading to higher entropy, whereas at lower temperatures hydrogen bonding of the hexamer to waters in other hexamers (enthalpy) becomes more important.

■ ASSOCIATED CONTENT

Ⓢ Supporting Information

Detailed calculation method and calculated power spectrum for other models. Additional data for the power spectra of librational densities and structural analyses. This material is available free of charge via the Internet at http://pubs.acs.org/.

■ AUTHOR INFORMATION

Corresponding Author

*E-mail: wag@wag.caltech.edu.

Present Address

‖J.J.: Department of Chemistry, University of Chicago, 5735 South Ellis Avenue, Chicago, Illinois 60637, United States.

Notes

The authors declare no competing financial interest.

■ ACKNOWLEDGMENTS

This project was carried out by J.J. at KAIST as part of a course that W.A.G. taught during fall 2013. We thank Prof. Hyungjun Kim for the use of his computer clusters for these calculations. Some support was provided by DARPA (HR0011-14-2-0003).

■ REFERENCES

(1) Jeng, M. The Mpemba effect: When can hot water freeze faster than cold? *Am. J. Phys.* **2006**, *74*, 514.

(2) Auerbach, D. Supercooling and the Mpemba effect: When hot water freezes quicker than cold. *Am. J. Phys.* **1995**, *63*, 882−885.

(3) Moore, E. B.; Molinero, V. Structural transformation in supercooled water controls the crystallization rate of ice. *Nature* **2011**, *479*, 506−508.

(4) Russo, J.; Tanaka, H. The microscopic pathway to crystallization in supercooled liquids. *Sci. Rep.* **2012**, *2*, 505-1-8.

(5) Esposito, S.; De Risi, R.; Somma, L. Mpemba effect and phase transitions in the adiabatic cooling of water before freezing. *Phys. A (Amsterdam, Neth.)* **2008**, *387*, 757−763.

(6) Huang, Y.; Zhang, X.; Ma, Z.; Li, W.; Zhou, Y.; Zhou, J.; Zheng, W.; Sun, C. Q. Size, separation, structural order, and mass density of molecules packing in water and ice. *Sci. Rep.* **2013**, *3*, 3005-1-5.

DOI: 10.1021/jp511752n
J. Phys. Chem. C 2015, 119, 2622−2629

(7) Molinero, V.; Moore, E. B. Water Modeled As an Intermediate Element between Carbon and Silicon. *J. Phys. Chem. B* **2008**, *113*, 4008−4016.
(8) Berendsen, H. J. C.; Postma, J. P. M.; van Gunsteren, W. F.; Hermans, J. In *Intermol. Forces*; Pullman, B., Ed.; D. Reidel Publishing Company: Dordrecht, 1981; pp 331−342.
(9) Levitt, M.; Hirshberg, M.; Sharon, R.; Laidig, K. E.; Daggett, V. Calibration and testing of a water model for simulation of the molecular dynamics of proteins and nucleic acids in solution. *J. Phys. Chem. B* **1997**, *101*, 5051−5061.
(10) Plimpton, S. Fast parallel algorithms for short-range molecular dynamics. *J. Comput. Phys.* **1995**, *117*, 1−19.
(11) Hobbs, P. V. *Ice Physics*; Clarendon Press: Oxford, 1974.
(12) Lobban, C.; Finney, J.; Kuhs, W. The structure of a new phase of ice. *Nature* **1998**, *391*, 268−270.
(13) Sanz, E.; Vega, C.; Abascal, J.; MacDowell, L. Phase diagram of water from computer simulation. *Phys. Rev. Lett.* **2004**, *92*, 255701.
(14) Lin, S.-T.; Blanco, M.; Goddard, W. A., III. The two-phase model for calculating thermodynamic properties of liquids from molecular dynamics: Validation for the phase diagram of Lennard−Jones fluids. *J. Chem. Phys.* **2003**, *119*, 11792.
(15) Lin, S.-T.; Maiti, P. K.; Goddard, W. A., III Two-Phase Thermodynamic Model for Efficient and Accurate Absolute Entropy of Water from Molecular Dynamics Simulations. *J. Phys. Chem. B* **2010**, *114*, 8191−8198.
(16) Liu, H.; Wang, Y.; Bowman, J. M. Vibrational Analysis of an Ice Ih Model from 0 to 4000 cm^{-1} Using the Ab Initio WHBB Potential Energy Surface. *J. Phys. Chem. B* **2013**, *117*, 10046−10052.
(17) Wang, Y.; Shepler, B. C.; Braams, B. J.; Bowman, J. M. Full-dimensional, ab initio potential energy and dipole moment surfaces for water. *J. Chem. Phys.* **2009**, *131*, 054511.
(18) Bertie, J.; Whalley, E. Infrared Spectra of Ices II, III, and V in the Range 4000 to 350 cm^{-1}. *J. Chem. Phys.* **1964**, *40*, 1646.
(19) Bertie, J.; Whalley, E. Optical Spectra of Orientationally Disordered Crystals. II. Infrared Spectrum of Ice Ih and Ice Ic from 360 to 50 cm^{-1}. *J. Chem. Phys.* **1967**, *46*, 1271.
(20) Mpemba, E. B.; Osborne, D. G. Cool? *Phys. Educ.* **1969**, *4*, 172.
(21) Smolin, N.; Daggett, V. Formation of Ice-like Water Structure on the Surface of an Antifreeze Protein. *J. Phys. Chem. B* **2008**, *112*, 6193−6202.
(22) Longinotti, M. P.; Carignano, M. A.; Szleifer, I.; Corti, H. R. Anomalies in supercooled NaCl aqueous solutions: A microscopic perspective. *J. Chem. Phys.* **2011**, *134*, 244510.
(23) Li, T.; Donadio, D.; Galli, G. Ice nucleation at the nanoscale probes no man's land of water. *Nat. Commun.* **2013**, *4*, 1887.
(24) Malaspina, D. C.; Bermúdez di Lorenzo, A. J.; Pereyra, R. G.; Szleifer, I.; Carignano, M. A. The water supercooled regime as described by four common water models. *J. Chem. Phys.* **2013**, *139*, 024506.
(25) McQuarrie, D. A *Statistical Mechanics*; Harper & Row: New York, 1976.
(26) Futamura, R.; Iiyama, T.; Hamasaki, A.; Ozeki, S. Negative thermal expansion of water in hydrophobic nanospaces. *Phys. Chem. Chem. Phys.* **2011**, *14*, 981−986.

DOI: 10.1021/jp511752n
J. Phys. Chem. C 2015, 119, 2622−2629